Journal of Materials Chemistry A

ROYAL SOCIETY OF CHEMISTRY

PAPER

View Article Online
View Journal | View Issue

Cite this: J. Mater. Chem. A, 2022, 10, 25078

A black energy-saving electrochromic device based on a dye copolymer–metal complex†

Ruipeng Shen, Haozhe Xi, Yuyang Wang, Guozhu Ren, Duo Liu, Yu-Mo Zhang * and Sean Xiao-An Zhang *

Received 25th August 2022
Accepted 1st November 2022

DOI: 10.1039/d2ta06749h

rsc.li/materials-a

Bistable black electrochromic (EC) devices have attracted increasing attention of researchers due to their ultra-low energy consumption and tunable sunlight penetration in the visible region. However, unsatisfactory optical performance and color stability limit their development and application in smart windows and non-emissive displays. In this work, aiming at the problems of poor dynamic coordination, and insufficient stability between copper ions and dye molecules, a copolymer containing a dye and cuprous complex has been designed and synthesized for a black bistable EC material with energy-saving properties. Based on this, a semi-solid black EC prototype device with bistable ability (maintains the color state for 2 h after electric stimulation) and high contrast ratio has been fabricated and demonstrated. The method proposed and verified here is applicable to other dye molecules with similar functional groups, thereby realizing energy-saving and multicolor display.

Introduction

Electrochromism refers to a phenomenon of optical manipulation through electric stimulation.[1] Numerous kinds of electrochromic materials such as inorganic electrochromic materials,[2] organic electrochromic materials[3–7] and metal–organic electrochromic materials[8–12] have been reported. Hereinto, bistable electrochromic materials and devices attract lots of attention because they can possess two or more stable optical states that can be reversibly switched by electrical stimulation. Compared with commercial display technology such as liquid crystal display (LCD), bistable electrochromic displays could retain information without energy consumption.[13,14] Due to the advantages of ultra-low energy consumption and long-term maintenance of expected color/transmittance, bistable electrochromic devices have broad application prospects[15–17] in smart windows,[18–21] non-emission displays,[22] *etc.* As one of the most important parts of optical model and display technology, bistable black electrochromic devices can adjust the intensity and spectrum of the entire visible region of solar light and has been expected by many research groups. In recent years, organic molecules[23] or polymers,[24–26] metal oxides[27,28] and hybrid materials[29,30] have been used to fabricate electrochromic black devices. The related reaction mechanisms can be attributed to color-mixing,[31,32] electrodeposition,[33–35] the designing of new materials, *etc.* For example, black electrochromic devices were prepared by mixing three different colored functionalized POSSs, namely octaviologen (OHV-POSS), thiophene (OTxHV-POSS) and phenyl (OphHV-POSS).[31] TiO_2-supported viologen and triphenylamine derivatives were designed to fabricate black electrochromic devices.[29] And a new black electrochromic device was achieved by electrodeposition of metal elements such as Cu and Bi.[35] However, few of them were reported with satisfying bistability, which has greatly limited the application of electrochromic materials and devices into the above-mentioned areas and energy-saving optical modulation.

Recently, we used dynamic metal–ligand interaction to design and synthesize new electrochromic materials. Based on this strategy, the color of switchable dyes (such as molecular probes for metal ion and pH-sensitive molecules) can be changed reversibly by regulating the valence of metal ions through electrical stimulation. And a series of new electrochromic devices with different colors had been prepared by mixing different switchable dyes or polymers. However, it is hard to balance the optical tunability and bistable properties due to the limited solubility and intermiscibility of metal ions and switchable dyes in this mixed strategy (Fig. 1a). For example, a higher optical tunability (74% transmittance change) can be obtained in a liquid device owing to the good solubility of the metal ions and switchable dyes, but intrinsic diffusion limits the bistability of liquid devices (no retention time).[36] Although a better bistability (1.5 h retention time) can be observed in a semi-solid device with a mixture of polymerized switchable dyes and the metal ionic ligand polymer, the intermiscibility of the two polymers restricted the optical tunability (about 21.4% transmittance change)[37] (Fig. 1b). Thus, breaking the limit of the mixed strategy is key to design

State Key Lab of Supramolecular Structure and Materials, College of Chemistry, Jilin University, 130012 Changchun, P. R. China. E-mail: zhangyumo@jlu.edu.cn

† Electronic supplementary information (ESI) available. See DOI: https://doi.org/10.1039/d2ta06749h

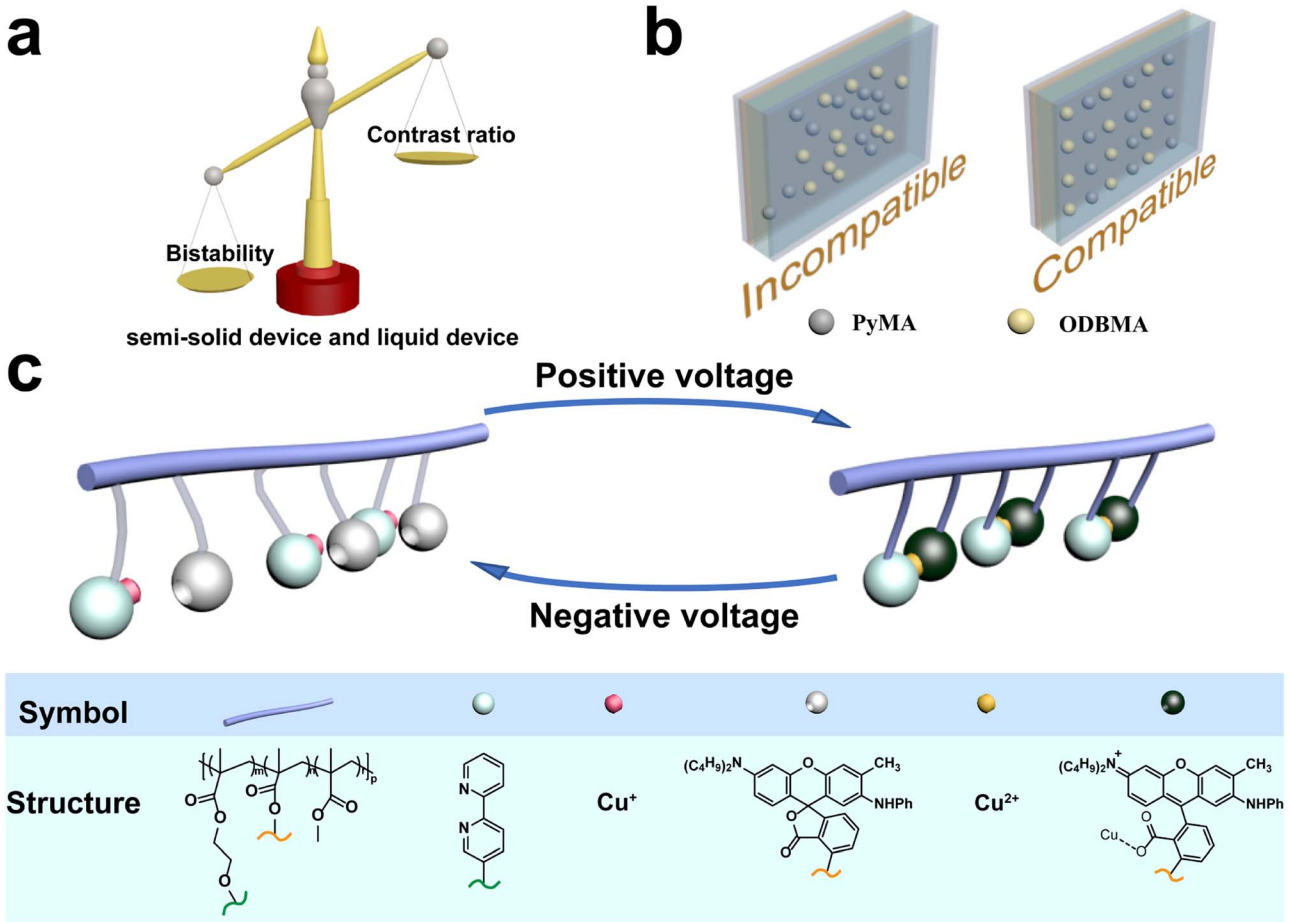

Fig. 1 (a) Imbalance between bistability and the contrast ratio of the semi-solid device and liquid device, (b) the difference between electrochromic devices based on two components and a single component, and the structure of ODBMA and PyMA can be found in ESI Fig. S1.† (c) Mechanism of color-changing and color-bleaching processes.

a bistable black electrochromic device with higher optical tunability and longer retention time.

In this work, a copolymer ODB–Py(CuCl)–MA (M10) containing dye molecules 2-anilino-6-(dibutylamino)-3-methylfluoran (ODB-2) and a cuprous complex has been designed and synthesized through radical polymerization (Fig. 1c). The structure and color-changing mechanism of the material were confirmed by cyclic voltammetry (CV), ultra-violet visible spectrophotometry (UV-Vis), Fourier-transform infrared spectroscopy (FT-IR) and X-ray photoelectron spectroscopy (XPS).And then, a device based on copolymer M10 has been fabricated with a high contrast ratio (37% transmittance change), good bistability (maintains the color state without electric stimulation after 2 h), and satisfying cycle stability (more than 500 times). We believe this material can provide researchers with new ideas to break the bottle neck of black energy-saving electrochromic devices.

Results and discussion

Design and synthesis

As we mentioned above, to design black-color electrochromic materials based on a dynamic coordination copolymer, suitable dye molecules and metal ions should be chosen wisely (Text S3†). A 2-anilino-6-(dibutylamino)-3-methylfluoran (ODB-2) derivative was used as dye molecules in the copolymer due to its deep dyeing, black color, good light fastness and good structure stability when used as a heat sensitive dye for thermosensitive paper. Cuprous ions were introduced through coordination reaction between cuprous chloride and bipyridine in the copolymer. The synthesis route of the coordination copolymer is shown in Scheme 1, and reaction details, structure characterization studies and the synthesis route of the contrast molecule can be found in the ESI (Text S1, S2 and S4†).

To demonstrate the structure of M10, Fourier transform infrared spectroscopy (FT-IR) (Fig. 2a and b), X-ray photoelectron spectroscopy (XPS) (Fig. 2d and e), scanning electron microscopy (SEM) (Fig. 2f) and energy dispersive X-ray spectroscopy (EDX) (Fig. 2g–i) have been performed. As shown in Fig. 2a and S2,† there are two doublet peaks at about 1435 cm^{-1}, 1456 cm^{-1} and 1558 cm^{-1}, 1575 cm^{-1} of M9, which can be confirmed as stretching vibrational absorption of the bipyridine skeleton through a previous work.[37] The shape and position of these doublets change after cuprous coordination with bipyridine (M10) as shown in Fig. 2a. The same changes can also be found between the molecule bipyridine (BiPy) and complex

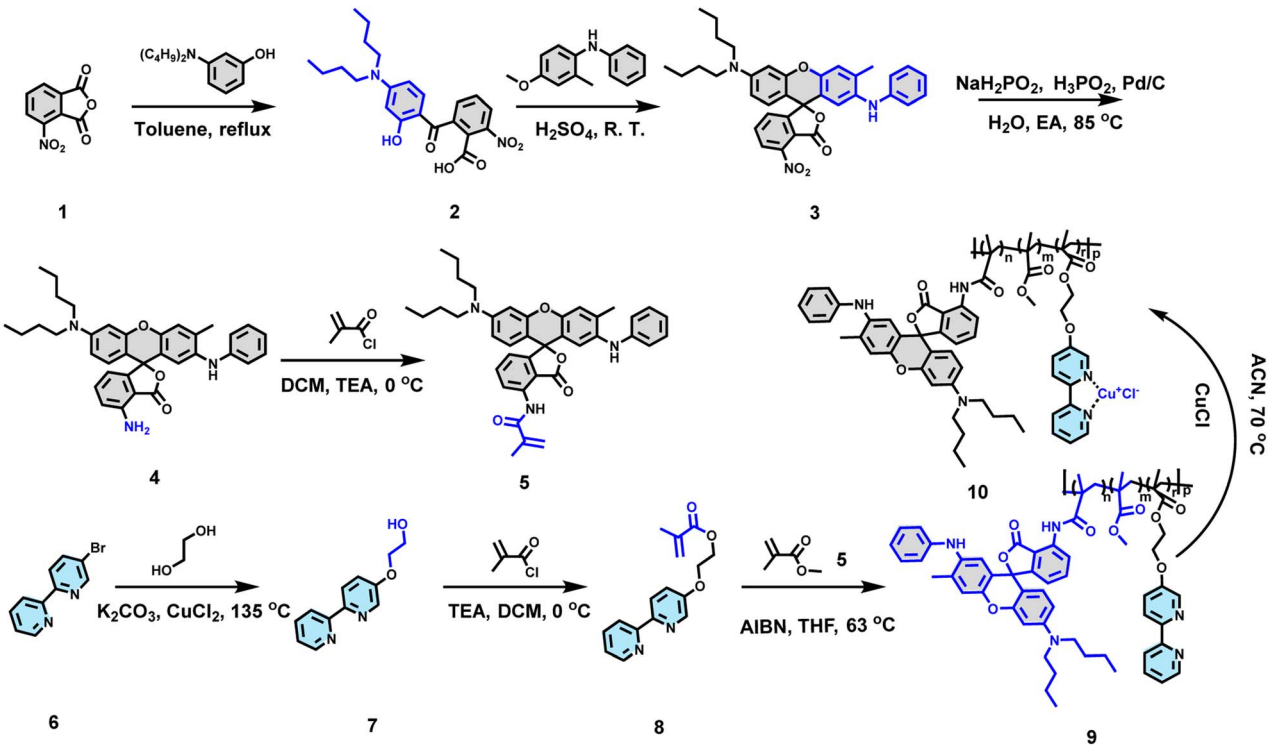

Scheme 1 Synthesis route of M10. EA: ethyl acetate, TEA: triethylamine, DCM: dichloromethane, AIBN: 2,2′-azobis(2-methylpropionitrile), THF: tetrahydrofuran, and ACN: acetonitrile. The grey hexagon refers to the dye part in the molecule, the blue hexagon refers to the bipyridine part in the molecule, and the blue line refers to the new part of the compound.

bipyridine–CuCl (BiPy–CuCl), as shown in Fig. 2b. These differences can be attributed to changes in the electron density of the pyridine backbone after coordination (Fig. 2c). It means that cuprous ions are coordinated with bipyridine in M10.

As shown in Fig. 2d and e, binding energy of the nitrogen 1s electron in M9 was measured by XPS. For M9, XPS spectra of N could be divided into two parts, N of bipyridine at about 398.7 eV, and N of amine at about 399.4 eV. For M10, binding energy spectra of N could belong to N of amine at 399.4 eV and N of bipyridine at 399.6 eV. The shift in binding energy of N for bipyridine might be because electrons of bipyridine was seized by cuprous ions, which indicated that CuCl has been coordinated with bipyridine. Besides, signals of N (Fig. 2g), Cu (Fig. 2h) and C (Fig. 2i) in EDX graphs of M10 films were evenly distributed, which means that the Cu element has been introduced into polymer. Thus, coordination between cuprous ions and bipyridine can be confirmed and M10 had been synthesized successfully.

Feasibility and mechanism

Then, the electrochromic feasibility of the dye copolymer was investigated. Two new absorption peaks at about 590 nm and 465 nm appeared after the colorless solution of M10 was stimulated by a positive voltage (+1.1 V) as shown in Fig. 3a. Interestingly, those two new peaks are similar to those of function dye ODB coordinated with cupric ions when copper chloride was added to M10 solution. These phenomena revealed that this copolymer exhibits electrochromic properties, and the color change may be due to the copper ion generated by the redox of cuprous ion. To prove this conjecture, the absorption spectra of M9 and CuCl as the reference molecule (Fig. 3b) were measured. Before and after the same stimulation, M9 solution exhibited no absorption peak in the visible region from 400 to 800 nm. And the absorption of colorless CuCl solution has increaed at 400 nm after 1.1 V stimulation, because Cu^{2+} was generated by the oxidation of CuCl. It means that the color change cannot be observed when CuCl or M9 is alone. Thus, we can speculate that the color change of M10 may be due to the coordination between ODB and cupric ions generated by the oxidation of cuprous ions.

As we mentioned above, cuprous ions should be oxidized first, and then coordinate with dye molecules. It means that the oxidation potential of cuprous chloride should be below than that of ODB as shown in ESI Fig. S3.† To prove our assumption, cyclic voltammetry (CV) curves and *in situ* absorption spectra were obtained to analyse the redox properties of M9, M10 and CuCl (Fig. 3c). The oxidation potential of M10 and BiPy–CuCl (0.5 V in ESI Fig. S4†) is lower than that of M9 (above 0.7 V), which confirms that CuCl is oxidized first in M10. To estimate the electrochromic process mechanism of M10, the absorbance of M9, M10 and CuCl at 590 nm, which is characteristic absorption of ODB, were detected by *in situ* absorption spectra (Fig. 3c). Both CuCl and M9 show no absorption changes during −0.3 V to 0.9 V. Nevertheless, absorbance for M10 increased with the increase in potential, then decreased with the decrease

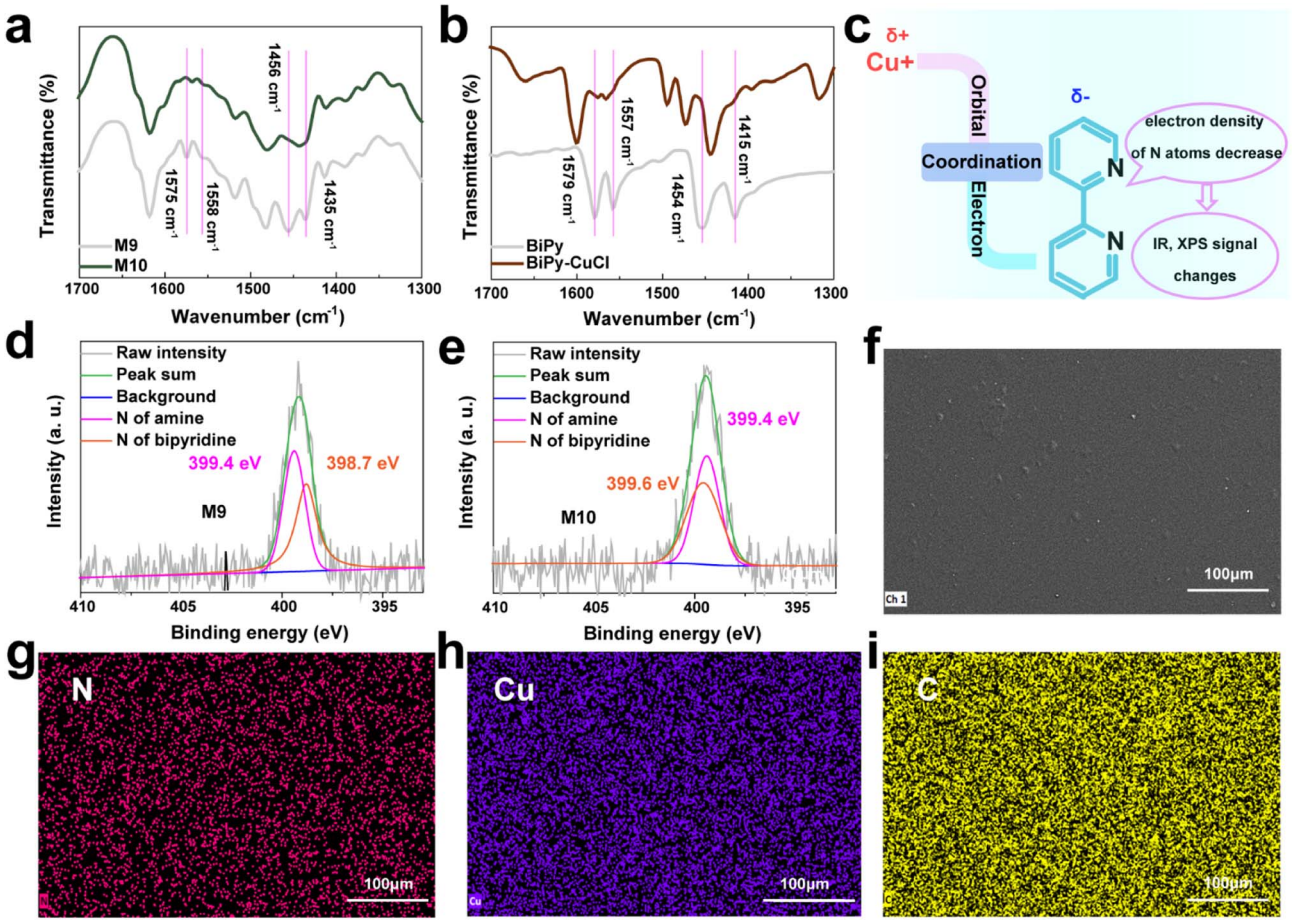

Fig. 2 (a) Fourier transform infrared spectroscopy of M9 (light gray) and M10 (dark green). (b) Fourier transform infrared spectroscopy of bipyridine (Bipy, light grey) and the complex of bipyridine and cuprous chloride (Bipy–CuCl, brown). (c) Schematic of XPS, and the FT-IR spectrum changing mechanism. (d) and (e) XPS spectra of N atom of M9 (d) and M10 (e). (f) SEM of the M10 film, (g)–(i) EDX spectra of N (g), Cu (h), and C (i) in the M10 film.

in potential, and returned to the initial state when the potential was scanned to the open-circuit voltage. The result indicated that the reversible color change of M10 is due to the reversible generation of cupric ions and dynamic coordination between ODB and copper adjusted by the stimulating voltage.

Based on the above conjecture, M10 would be oxidized as M11 (ODB–Py($CuCl_2$)–MA, Text S4†). To prove this mechanism, X-ray photoelectron spectroscopy of M9 (Fig. 2d 3d), M10 with (Fig. 3f) and without electric stimulation (Fig. 2e 3e) and M11 (Fig. 3g) has been performed. Similar to M9 (Fig. 3d), the intensity of O in M10 (Fig. 3e) could be divided into C–O (531.9 eV) and C=O (533.4 eV), which matches our assumption that ODB has no obviously interaction with cuprous ions. However, the intensity of M10 after electric stimulation could be assumed to be the sum of three peaks (Fig. 3f) containing C–O (531.9 eV), C=O (533.4 eV) and C–O–Cu (533.2 eV) by comparison with that of M11 (Fig. 2g). These same peaks show obvious interactions between ODB and cupric ions when M10 was stimulated by electricity. Meanwhile, the binding energy of N in M11 (ESI Fig. S5†) is almost similar to that in M10 (Fig. 2e), which shows that cupric ions still interacted with bipyridine. These results reveal that both pyridine and ODB are coordinated with cuprous ions after electric stimulation, and the mechanism is like that shown in Fig. 3h.

Performance of the solid device

After investigating the electrochromic feasibility and mechanism of the dye copolymer containing the cuprous complex M10, a semi-solid multilayer device containing an electrochromic layer, ion conductive layer and ion storage layer was fabricated by blade coating. And the detailed process of device preparation is shown in the ESI (Text S6 and Fig. S6†). As shown in Fig. 4a, this multilayer device is pale yellow and transparent, and no obvious absorption peak can be observed in the 500–800 nm range of the transmission spectrum. When a positive voltage of about +1.0 V was applied, new absorption peaks at about 590 nm and 450 nm appeared along with the color change of the device from pale yellow to black. Furthermore, the transmission spectrum of the M10 device can change back into the initial state and the color change returned reversibly to the initial state at −0.8 V, which means that this device exhibits wonderful electrochromic properties.

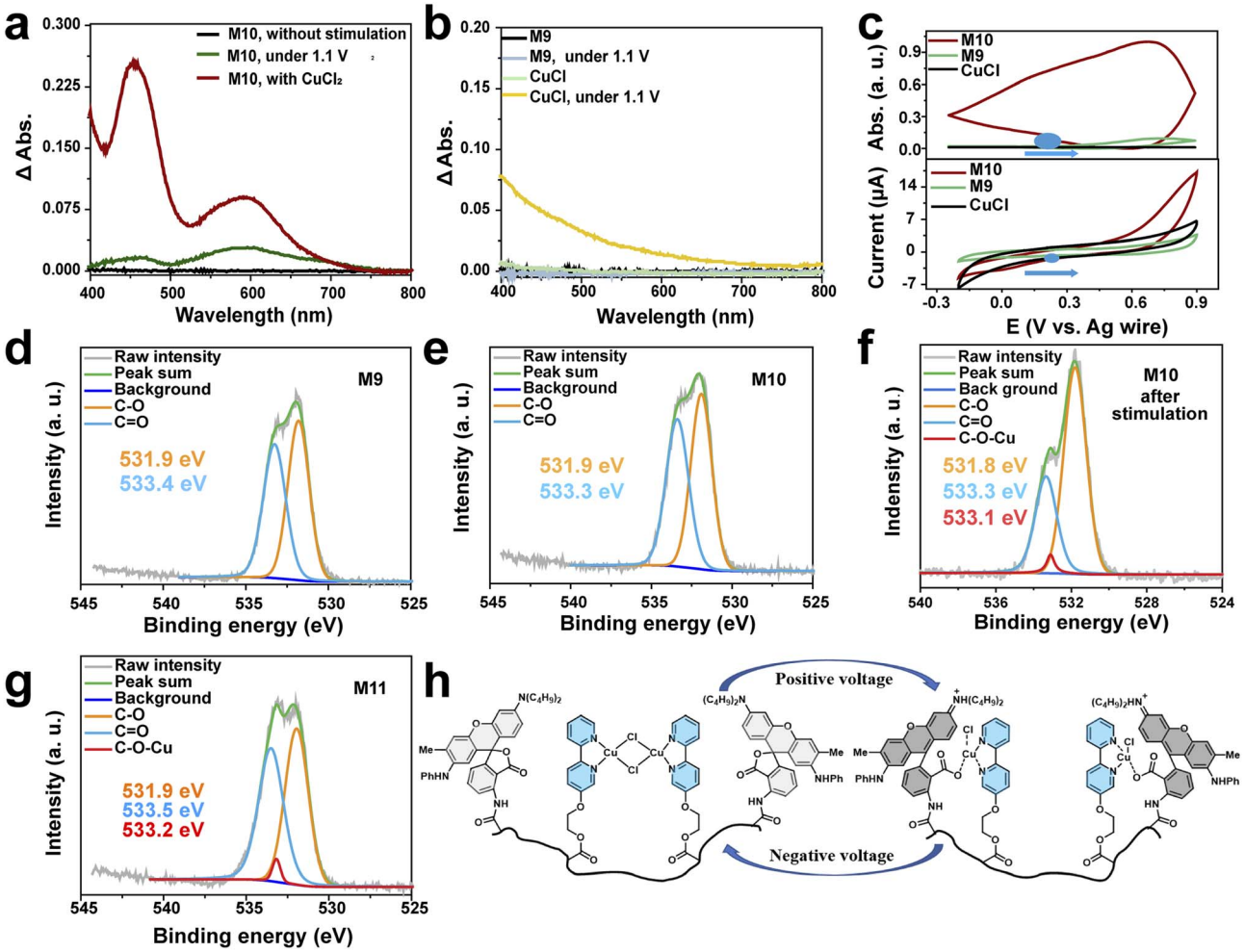

Fig. 3 (a) Ultraviolet-visible spectrum of M10 without stimulation (black), at 1.1 V (dark green) and stimulated by 1.8 eq. $CuCl_2$ (brown). (b) Ultraviolet-visible spectrum of M9 without stimulation (black) and at 1.1 V (light blue) and CuCl (light green) without stimulation and at 1.1 V (yellow). (c) *In situ*-cyclic voltammetry-ultraviolet-visible spectrum of M10 (brown), M9 (green), and CuCl (black), (d) XPS spectrum of O in M9, (e) XPS spectrum of O in M10, and (f) XPS spectrum of O in M10 after stimulation. (g) XPS spectrum of O in M11. (h) Mechanism of M10 color change at a positive voltage. Grey hexagons refer to aromatic rings belonging to ODB, and cyan hexagons refer to aromatic rings belonging to pyridine. The curve refers to the polymer backbone of M10.

To obtain the best electrochromic performance, the structure of M10 consisting of three functional units should be optimized to balance the film-forming properties and electrochromic properties. For the dye copolymer containing the cuprous complex M10, each unit has its own function. By increasing the ratio of MMA as the polymer backbone, film-forming ability of the copolymer will be enhanced. By increasing the ratio of dye ODB and cuprous complex Py(CuCl) as the function unit, the electrochromic properties of the copolymer will be improved. Four copolymers M10 with different MMA ratios have been synthesized, and their ratios were confirmed by using the ^{1}H NMR spectra (ESI Fig. S7–S11†).

To investigate the film-forming ability of these copolymers with different MMA ratios, their films were fabricated by blade coating and tested by Scanning electron microscopy (SEM) (Fig. 4b, c, e and f). As we expected, the copolymer with a higher MMA ratio is smoother than that with a lower ratio, and copolymer ODB : Py(CuCl) : MA = 1 : 2 : 20 and copolymer ODB : Py(CuCl) : MA = 1 : 2 : 40 are smooth enough. Hereinto, copolymer ODB : Py(CuCl) :MA = 1 : 2 : 20 was chosen due to its higher ratio of the dye and cuprous complex. Except for the MMA ratio, the thickness of the electrochromic layer is also a crucial parameter for the electrochromic device, which can affect both the change intensity of absorbance at 590 nm and optical maintain time. As depicted in Fig. 4d, the change intensity of absorbance increased with the increase in the thickness from 0.36 μm to 2.78 μm. However, the optical maintain time of the device increased first and then decreased. And the device with a 1.9 μm film shows longest optical maintain time and highest change intensity of absorbance.

After the optimization of parameters, the performance of the device in terms of turn on voltage, bistable performance and cycling stability was investigated. As shown in Fig. 4g, the transmittance change of the device at 590 nm increased with the increasing stimulated voltage. And the change could be detected when +0.3 V was applied, which indicated that the

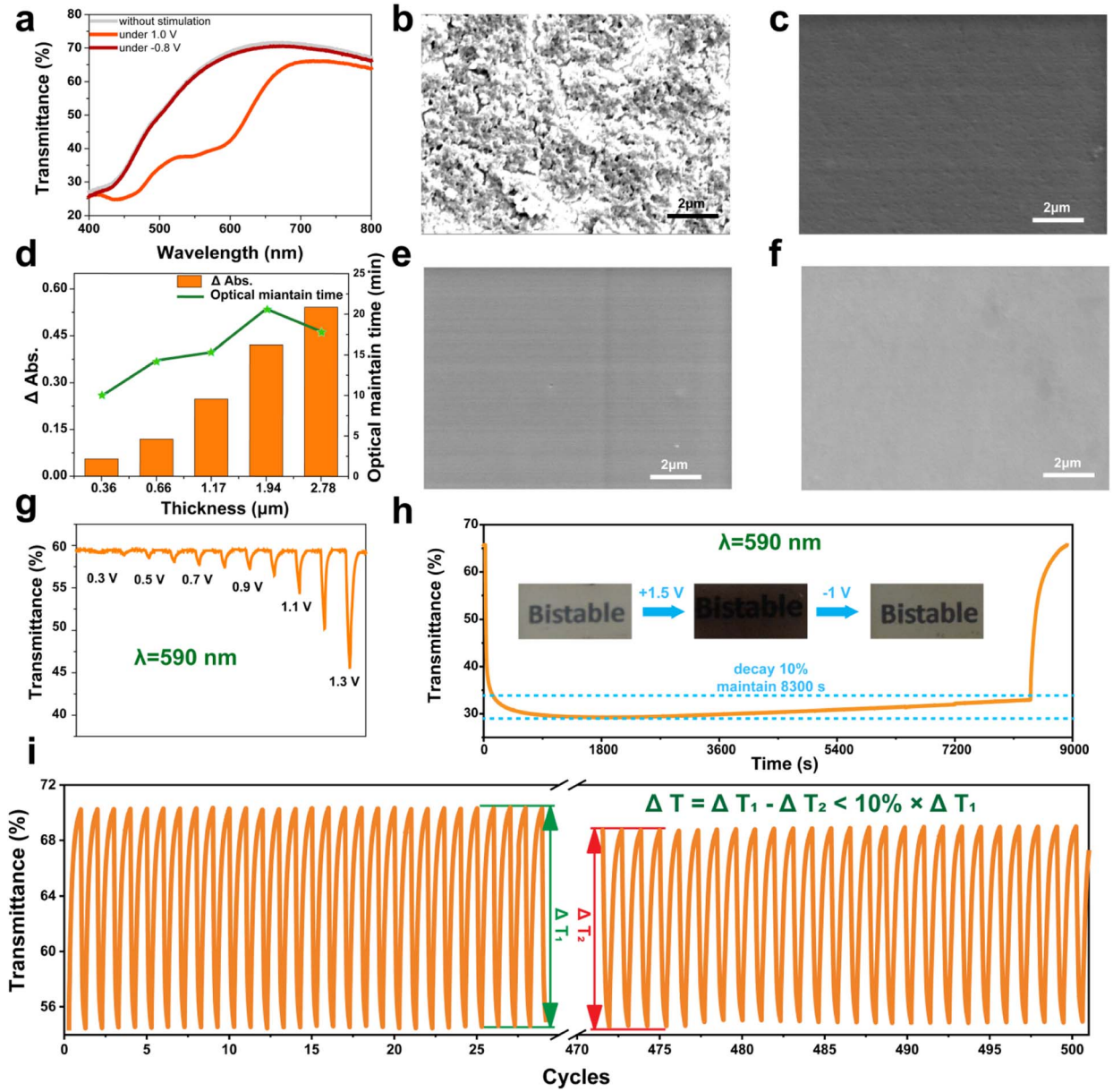

Fig. 4 (a). Ultraviolet-visible spectrum of the black electrochromic device based on M10. SEM photos of the electrochromic layer of M10 with the different ratios of ODB : Py : MA as 1 : 2 : 3 (b), 1 : 2 : 8 (c), 1 : 2 : 20 (e), and 1 : 2 : 40 (f), respectively. (d). Variation of absorption and colored-state maintain time (optical maintain time) of devices with electrochromic layers of different thicknesses. (g) The transmittance at 590 nm of the device stimulated with different voltages. (h) The transmittance at 590 nm of the device at 1.5 V 15 s, and photos of the device are inserted. (i) Cycling stability of the electrochromic device; the wavelength was set as 590 nm.

turn-on voltage of the electrochromic device is about 0.3 V. Another important ability of the electrochromic device is optical maintain time of the color state. The transmittance of the device changes to 29% from 66% at 1.5 V for 15 s, and the attenuation of optical intensity is less than 10% after 2 h without stimulation (Fig. 4h). Although the de-color progression of the device caused by diffusion of the substances from the ion storage layer still exists, the result still shows a satisfying bistable property in this device. The high contrast ratio and good bistable performance indicated that the M10 electrochromic device has potential applications in energy-saving electrochromic devices and display. Furthermore, this device can switch from the pale yellow state to color state more than 500 times with low damping (less than 10%) (Fig. 4i).

Conclusions

In this work, a new copolymer containing a dye and cuprous complex has been designed and synthesized to balance the optical tunability and bistable properties of the black energy-saving electrochromic material and device. And its dynamic metal–ligand interaction has been confirmed by the cyclic

voltammetry test, ultra-violet visible spectrophotometer tests, Fourier-transform infrared spectroscopy tests, and X-ray photoelectron spectroscopy. More importantly, the semi-solid black electrochromic device exhibited long optical maintain time (2 h), high contrast ratio and satisfactory cyclic reversibility (more than 500 cycles). Moreover, this synthesis routine is suitable for other molecules with similar functional groups; therefore, multi-color electrochromic devices can be achieved. We believe this synthesis route and electrochromic mechanism can provideanother way to realize energy-saving display and enrich the field of optical modulation.

Author contributions

Ruipeng Shen, Yu-Mo Zhang and Sean Xiao-An Zhang designed the studies and wrote the paper. Ryupeng Shen, Guozhu Ren, Yuyang Wang, Duo Liu and Haozhe Xi performed most of the experiments. Ruipeng Shen, Yu-Mo Zhang and Sean Xiao-An Zhang performed data analysis. All authors discussed the results and commented on the manuscript.

Conflicts of interest

There are no conflicts to declare.

Acknowledgements

This study was supported by the National Natural Science Foundation of China (Grant No. 22075098), the Natural Science Foundation of Jilin Province (CN) (No. 20210101133JC), the Key Lab of Advanced Optical Manufacturing Technologies of Jiangsu Province & Key Lab of Modern Optical Technologies of Education Ministry of China (Soochow University, no. KJS1911) and the Fundamental Research Funds for the Central Universities.

Notes and references

1 G. Cai, J. Wang and P. S. Lee, *Acc. Chem. Res.*, 2016, **49**, 1469.
2 J. Chen, *et al.*, *Adv. Mater.*, 2021, **33**, 2007314.
3 H. Shin, S. Seo, C. Park, N. Jongbeom, M. Han and E. Kim, *Energy Environ. Sci.*, 2016, **9**, 117.
4 X. Tu, X. Fu and Q. Jiang, *Displays*, 2010, **31**, 150.
5 Q. Jiang, F. Liu, T. Li and T. Xu, *J. Mater. Chem. C*, 2014, **2**, 618.
6 A. A. Argun, C. Ali and J. R. Reynolds, *Adv. Mater.*, 2003, **15**, 1338.
7 S. Macher, *et al.*, *Adv. Funct. Mater.*, 2020, **30**, 1906254.
8 M. Lahav and M. E. van der Boom, *Adv. Mater.*, 2018, **30**, 1706641.
9 K. Takada, R. Sakamoto, S.-T. Yi, S. Katagiri, T. Kambe and H. Nishihara, *J. Am. Chem. Soc.*, 2015, **137**, 4681.
10 C.-W. Kung, *et al.*, *Chem. Mater.*, 2013, **25**, 5012.
11 R. Sydam and M. Deepa, *J. Mater. Chem. C*, 2013, **1**, 7930.
12 G. Cai, *et al.*, *ACS Energy Lett.*, 2020, **5**, 1159.
13 C. Gu, A.-B. Jia, Y.-M. Zhang and S. X.-A. Zhang, *Chem. Rev.*, 2022, **122**, 1467.
14 Y. Wang, H. Nie, J. Han, Y. An, Y.-M. Zhang and S. X.-A. Zhang, *Light: Sci. Appl.*, 2021, **10**, 33.
15 K. Xiong, O. Olsson, J. Svirelis, C. Palasingh, J. Baumberg and A. Dahlin, *Adv. Mater.*, 2021, **33**, 2103217.
16 Z. Wang, X. Wang, S. Cong, F. Geng and Z. Zhao, *Mater. Sci. Eng., R*, 2020, **140**, 100524.
17 V. K. Thakur, G. Ding, J. Ma, P. S. Lee and X. Lu, *Adv. Mater.*, 2012, **24**, 4071.
18 J.-L. Wang, *et al.*, *Nano Lett.*, 2021, **21**, 9976.
19 H. Shin, S. Seo, C. Park, N. Jongbeom, M. Han and E. Kim, *Energy Environ. Sci.*, 2016, **9**, 117.
20 M. Son, D. Shin and C. S. Lee, *Adv. Mater. Interfaces*, 2021, **8**, 2001416.
21 A. Llordés, G. Garcia, J. Gazquez and D. J. Milliron, *Nature*, 2013, **500**, 323.
22 Y. Wang, *et al.*, *Nat. Mater.*, 2019, **18**, 1335.
23 I. Jang Ko, J. H. Park, G. W. Kim, L. Raju and J. H. Kwon, *Adv. Mater. Interfaces*, 2019, **6**, 1900710.
24 M. T. Otley, Y. Zhu, X. Zhang, M. Li and G. A. Sotzing, *Adv. Mater.*, 2014, **26**, 8004.
25 Q. Zhang, C.-Y. Tsai, L.-J. Li and D.-J. Liaw, *Nat. Commun.*, 2019, **10**, 1239.
26 P. Shi, *et al.*, *Adv. Mater.*, 2010, **22**, 4949.
27 W. Cheng, J. He, E. Kevan, N. J. Dettelbach, J. Johnson, R. S. Sherbo and C. P. Berlinguette, *Chem*, 2018, **4**, 821.
28 C. Eyovge, *ACS Appl. Nano Mater.*, 2021, **4**, 8600.
29 Y. Alesanco, A. Viñuales, G. Cabañero, J. Rodriguez and R. Tena-Zaera, *Adv. Opt. Mater.*, 2017, **5**, 1600989.
30 F.-W. Li, T.-C. Yena and G.-S. Liou, *Electrochim. Acta*, 2021, **367**, 137474.
31 G. K. Pande, J. S. Heo, J. H. Choi, Yu S. Eom, J. Kim, S. K. Park and J. S. Park, *Chem. Eng. J.*, 2021, **420**, 130446.
32 H. Shin, *et al.*, *ACS Appl. Mater. Interfaces*, 2012, **4**, 185.
33 K. Sheng, B. Xue, J. Zheng and C. Xu, *Adv. Opt. Mater.*, 2021, **9**, 2002149.
34 M. Son, D. Shin and C. S. Lee, *Adv. Mater. Interfaces*, 2021, **8**, 2001416.
35 S. M. Islam, T. S. Hernandez, M. D. McGehee and C. J. Barile, *Nat. Energy*, 2019, **4**, 223.
36 Y. Wang, R. Shen, S. Wang, Q. Chen, C. Gu, W. Zhang, G. Yang, Q. Chen, Y.-M. Zhang and S. X.-A. Zhang, *Chem*, 2021, **7**, 1308.
37 Y. Wang, R. Shen, S. Wang, Y.-M. Zhang and S. X.-A. Zhang, *Adv. Mater.*, 2022, **34**, 2104413.

